Sporadic inclusion body myositis-derived myotube culture revealed muscle cell-autonomous expression profiles

Naoki Suzuki（✉ naoki@med.tohoku.ac.jp ）

Tohoku University Graduate School of Medicine

Makoto Kanzaki

Tohoku University

Masashi Koide

Tohoku University Graduate School of Medicine

Rumiko Izumi

Tohoku University Graduate School of Medicine

Ryo Fujita

Tohoku University Graduate School of Medicine

Tadahisa Takahashi

Tohoku University Graduate School of Medicine

Kazumi Ogawa

Tohoku University Graduate School of Medicine

Yutaka Yabe

Tohoku University Graduate School of Medicine

Masahiro Tsuchiya

Tohoku Fukushi University

Masako Suzuki

Tohoku University Graduate School of Medicine

Ryuhei Harada

Tohoku University Graduate School of Medicine

Akiyuki Ohno

Tohoku University Graduate School of Medicine

Hiroya Ono

Tohoku University Graduate School of Medicine

Naoko Nakamura

Tohoku University Graduate School of Medicine

Kensuke Ikeda

Tohoku University Graduate School of Medicine

Hitoshi Warita

Tohoku University Graduate School of Medicine

Shion Osana

Tohoku University Graduate School of Medicine

Yoshitsugu Oikawa

Tohoku University Graduate School of Medicine

Takafumi Toyohara

Tohoku University Graduate School of Medicine

Takaaki Abe

Tohoku University Graduate School of Medicine

Ryoichi Nagatomi

Tohoku University Graduate School of Medicine

Yoshihiro Hagiwara

Tohoku University Graduate School of Medicine

Masashi Aoki

Tohoku University Graduate School of Medicine

Abstract

Sporadic inclusion body myositis (sIBM) is a muscle disease in older people and is characterized by inflammatory cell invasion into intact muscle fibers and rimmed vacuoles. The pathomechanism of sIBM is not fully elucidated yet, and controversy exists as to whether sIBM is a primary autoimmune disease or a degenerative muscle disease with secondary inflammation. Previously, we established a method of collecting CD56-positive myoblasts from human skeletal muscle biopsy samples. We hypothesized that the myoblasts derived from these patients are useful to see the cell-autonomous pathomechanism of sIBM. With these resources, myoblasts were differentiated into myotubes, and the expression profiles of cell-autonomous pathology of sIBM were analyzed. Myoblasts from three sIBM cases and six controls were differentiated into myotubes. In the RNA-sequencing analysis of these "myotube" samples, 104 differentially expressed genes (DEGs) were found to be significantly upregulated by more than twofold in sIBM, and 13 DEGs were downregulated by less than twofold. For muscle biopsy samples, a comparative analysis was conducted to determine the extent to which "biopsy" and "myotube" samples differed. Fifty-three DEGs were extracted of which 32 (60%) had opposite directions of expression change (e.g., increased in biopsy vs decreased in myotube). Apolipoprotein E (apoE) and transmembrane protein 8C (TMEM8C) were commonly upregulated in muscle biopsies and myotubes from sIBM. ApoE and myogenin protein levels were upregulated in sIBM. Given that enrichment analysis also captured changes in muscle contraction and development, the triggering of muscle atrophy signaling and abnormal muscle differentiation via TMEM8C or myogenin may be involved in the pathogenesis of sIBM.

The presence of DEGs in sIBM suggests that the myotubes formed from sIBM-derived myoblasts revealed the existence of muscle cell-autonomous degeneration in sIBM. The catalog of DEGs will be an important resource for future studies on the pathogenesis of sIBM focusing on primary muscle degeneration.

Introduction

Sporadic inclusion body myositis (sIBM) is a clinicopathologically defined muscle disease of older people [1–3]. The pattern of the affected muscles including finger flexor and knee extensor and dysphagia are characteristic of sIBM [4]. Muscle biopsy of sIBM shows rimmed vacuoles and inflammatory cell invasion into non-necrotic muscle fibers [5]. The pathomechanism of sIBM is not fully elucidated yet.

Controversy exists as to whether sIBM is a primary autoimmune disease or a degenerative muscle disease with secondary inflammation. The involvement of interferon-gamma mediated signaling pathway[6], myeloid dendritic and plasma cells[7], and highly differentiated cytotoxic T cells[8] in sIBM pathology has been reported. Anti-cytosolic 5'-nucleotidase 1A autoantibodies are found in the serum of patients with sIBM[9]. However, sIBM is usually refractory to immunosuppressive therapy. Muscle degeneration is an important aspect of sIBM etiology [10].

Muscle biopsy is necessary for the diagnosis of sIBM [11,12]. The rest of the diagnostic samples can be used for research, such as in gene expression profiling; for example, gene sets to differentiate sIBM

biopsy samples from other myositis using support vector machine-learning system are revealed [13]. Other groups analyzed two microarray datasets[8,14] derived from the Gene Expression Omnibus database and picked-up genes as a hub of a pathological network[15]. As the pathology of sIBM shows the involvement of cells such as inflammatory cell infiltration, fibrosis, and adipose tissues [16,17], the expression data analysis might be confounded by non-muscle cells.

In 1994, ApoE immunoreactive deposits in rimmed vacuole was first reported in sIBM muscle biopsy [18]. ApoE and lipoprotein receptors are also found in rimmed vacuole structures, suggesting the aberrant cholesterol metabolism in sIBM muscles [19,20]. Amyloid beta-overexpressed mouse was used as the sIBM model[21]. The mechanisms of abnormal protein accumulation in muscle degeneration in sIBM are not well understood.

Previously, we established a method of collecting CD56-positive myoblasts from human skeletal muscles derived from muscle biopsy samples[22,23]. We hypothesized that the myoblasts derived from these patients are useful to see the cell-autonomous pathomechanism of sIBM. With these resources, we differentiated myoblasts into myotubes and analyze the expression profiles of the cell-autonomous pathology of sIBM.

Materials and Methods

Study population

The study protocol was approved by the Tohoku University Hospital's Institutional Review Board (Approval nos. 2014-1-703, 2016-1-884, 2019-1-493), and written informed consent was obtained from all participants.

Sample collection from patients with sIBM

From November 2015 to May 2018, we performed muscle biopsies on 13 patients who were presumptively diagnosed with sIBM. Muscle samples were collected from nine patients who agreed to undergo a biopsy. The number of patients evaluated was restricted because of the limited access to the fluorescence-activated cell sorting (FACS) system at our institute and the requirement for performing the procedure on the same day as the muscle biopsy.

The cells prepared from each muscle by FACS were separated into three replicates for characterization and culture. In each patient, muscle biopsy specimens (approximately 300 mg) were obtained from the muscle belly of the biceps brachii or lower proximal muscles (Table 1). Three lines of actively proliferating myoblasts were used for the analysis.

Sample collection from the control participants (patients with rotator cuff tears [RCT])

From January 2015 to December 2015, arthroscopic RCT repairs were performed in 42 patients who were unresponsive to conservative treatments [23]. Muscle samples were collected from 19 patients who agreed to undergo a biopsy. None of the patients had tears in the intact subscapularis (SSC) tendon based on both magnetic resonance imaging and arthroscopic findings. No patients had muscular disease, neurovascular disorders, paralysis, or trauma. Muscle biopsy specimens (approximately 300 mg) were obtained from the same portion of the muscle belly of the SSC in each patient who underwent arthroscopic surgery (Table 1)[23].

Primary myoblast isolation

Human satellite cells were isolated from the muscles of patients who agreed to undergo biopsy. All experiments were performed in accordance with relevant guidelines and regulations as described elsewhere [23,24]. Briefly, the tissue was minced and digested with 0.2% collagenase (Wako Pure Chemicals Industries) and 0.1% DNase I (Sigma-Aldrich, St. Louis, MO, USA), filtered through a 70-μm cell strainer (BD Biosciences, Franklin Lakes, NJ, USA), and centrifuged at 700 × g for 20 min. Pellets were resuspended in phosphate-buffered saline (PBS) containing 1% bovine serum albumin (BSA; Sigma-Aldrich) and then incubated with an Fc receptor blocking solution (Human TruStain FcX, 1:20 in the staining buffer; BioLegend, San Diego, CA, USA). Then, the samples were labeled with the following monoclonal antibodies (all from BioLegend and all at 1:20 dilution): fluorescein isothiocyanate (FITC)-conjugated anti-CD45 (clone HI30), FITC-conjugated anti-CD11b (clone ICRF444), FITC-conjugated anti-CD31 (clone WM59), phycoerythrin (PE)/Cy7-conjugated anti-CD34 (clone 581), allophycocyanin (APC)-conjugated anti-CD56 (clone MEM-188), and PE-conjugated anti-PDGFRα (clone 16A1). The negative set included blood markers CD11b and CD45 and endothelial markers CD31 and CD34. Although CD34 is expressed by the majority of mouse satellite cells[25], human muscle-derived CD34$^+$ cells are myogenic and adipogenic, whereas CD34$^-$ cells are myogenic but not adipogenic [26]. Therefore, CD34 was used as a negative selection marker. Human satellite cells were defined as single live mononuclear CD11b$^-$CD31$^-$CD34$^-$CD45$^-$CD56$^+$ cells. FACS was performed on a FACS ARIA II flow cytometer (BD Biosciences). Cells were seeded onto 24-well chamber slides coated with Matrigel (Dow Corning, Corning, NY, USA) in a growth medium containing DMEM/Ham's F10 mixture supplemented with 20% fetal bovine serum, 1% penicillin−streptomycin, 1% chicken embryonic extract (United States Biological, Salem, MA, USA), and 2.5 ng/mL basic fibroblast growth factor (Thermo Fisher Scientific, Waltham, MA, USA) and cultured at 37°C in a 5% CO_2 atmosphere. When cells reached 60−80% confluence, adherent cells were dissociated and split onto a new Matrigel-coated 15-cm dish to expand the activated satellite cells. Activated satellite cells (myoblasts) were suspended in Cell Banker (Takara, CB011, Japan) and stored in liquid nitrogen.

Cell culture

Human myoblasts were cultured using media purchased from Lonza (Walkersville, MD, USA). Three days after plating, the cells reached 80−90% confluence (day 0). Then, differentiation was induced by switching the growth medium to DMEM supplemented with 2% horse serum, 30 μg/mL penicillin, and 100

μg/mL streptomycin (differentiation medium). The differentiation medium was changed every 24 h during the 7–8 days of differentiation.

RNA extraction and sequencing analysis

Cultured myotubes were collected to extract the total RNA, which was performed using an RNeasy micro kit (Qiagen, Germany) according to the manufacturer's protocol. RNA-sequencing (RNA-seq) libraries were prepared using a TruSeq RNA-stranded mRNA Sample Prep Kit (Illumina, CA, USA). These libraries were clonally amplified on a flow cell and sequenced on a HiSeq2500 (HiSeq Control Software v2.2.58, Illumina) with a 51-mer single-end sequence. Image analysis and base calling were performed using Real-Time Analysis Software (v1.18.64, Illumina). For data analysis, UCSC hg19 and RefSeq were used as the reference human genome and gene model, respectively. For gene expression analysis, single-end reads were mapped to the human genome using TopHat (ver. 2.1.0) [27]. Cufflinks (ver. 2.2.1) was used to estimate the gene expression levels based on fragments per kilobase of the exon model per million mapped fragments [28]. Gene expression levels were compared between control cells and sIBM cells using Cuffdiff (ver. 2.2.1).

Immunohistochemistry and immunocytochemistry

The biopsy sections and cultured myotubes were washed with PBS and fixed for 20 min with 2% paraformaldehyde in PBS containing 0.1% Triton X-100. Samples were washed and blocked in PBS containing 5% CS and 1% BSA at room temperature. For immunofluorescence analysis, anti-desmin antibody (MAB-606102, DBS), ApoE (16H22L18, Invitrogen), dystrophin (NCL-Dys1, Leica), caveolin-3 (sc-55518, Santa Cruz), amyloid oligomers (A11; SPC-506D, StressMarQ), were used as the first antibody, and Alexa Fluor 488 or 568-conjugated anti-IgG was used as the secondary antibody, in a solution of 1% BSA in PBS. The samples were mounted on glass slides with Vectashield (Vector Laboratories, Burlingame, CA, USA) and observed with a confocal fluorescence microscope (Fluoview FV-1000; Olympus, Tokyo, Japan) or fluorescence microscope (BZ-X700; Keyence).

Immunoblotting

For immunoblot analysis, skeletal muscle protein was extracted from the human myotubes, as described previously [29]. Total cell proteins were extracted from cells with radio-immunoprecipitation buffer (ATTO) and measured using a Bicinchoninic Acid Kit (Thermo Fisher Scientific). After the adjustment of the protein concentration, protein samples were reacted with Laemmli buffer at 95°C for 5 min and separated by sodium dodecyl sulfate-polyacrylamide gel electrophoresis using 10–20% polyacrylamide gels (ATTO) under constant voltage of 200 V for 60 min. Then, the separated proteins were transferred to polyvinylidene difluoride membranes (Millipore, MA, USA). After blocking with 2% BSA (Pierce), membranes were probed with the indicated primary antibodies including ApoE (16H22L18, Invitrogen), myogenin (sc-12732, Santa Cruz), and GAPDH (2118L, CST) overnight at 4°C. Immunolabeling was visualized by incubation with horseradish peroxidase-linked secondary antibodies (5,000-fold dilution) at room temperature for 1 h, followed by treatment with an enhanced chemiluminescence prime reagent (GE

Healthcare, IL, USA); images were captured using an LAS-3000 Image Reader (Fujifilm, Tokyo, Japan). Blots were labeled with anti-GAPDH antibodies as the gel loading control.

Statistical analysis

Statistical analyses were performed using Student's t-test or analysis of variance with Tukey's multiple comparison test, and p-values < 0.05 indicated a statistically significant difference unless otherwise specified. Data are expressed as means ± SE unless otherwise specified.

Results

Myoblasts from three sIBM cases and six controls were differentiated into myotubes ("myotube": Table 1 and Fig. 1A). Immunocytochemistry revealed desmin-positive multinucleated myotubes after the differentiation in both groups (Fig. 1B–1E). RNA was extracted from these myotubes (Fig. 1A), and RNA-seq was performed (Fig. 2). In total, 104 genes were significantly upregulated by more than twofold in sIBM (Table 2). Myogenin[30] was upregulated in sIBM. Thirteen differentially expressed genes (DEGs) were downregulated by less than twofold (Table 3).

To broaden the range of genes, genes with a 1.5-fold or greater change were listed. In total, 991 genes were altered (Supplementary Table 1). Heat maps separated sIBM and control myotubes as expected (Fig. 2A). Gene Ontology (GO) term classification of genes with altered expression showed that pathways related to skeletal muscle function, such as muscle filament sliding and muscle contraction, were enriched in biological process (GO-BP). In molecular function (GO-MF), actin filament binding and structural constituents of muscle were also enriched (Fig. 2B, 2C). As expected, skeletal muscle cell-specific changes appear to be extracted.

To determine the extent to which the expression profiles found in these myotubes differed from those in the muscle biopsies, RNA-seq analysis was performed using muscle biopsy from sIBM (n = 3) and disease control (n = 4) samples ("biopsy" samples: Supplementary Table 2). Moreover, 901 genes showed more than 1.5-fold variation in the muscle biopsy samples. Proteasome (prosome and macropain) subunit, beta type, 8 (PSMB8), a member of the interferon-2 pathway, was increased, which correlated with previous analyses in the biopsied muscle [31]. The levels of other molecules in the interferon-2 pathway, namely, guanylate binding protein 1, interferon-inducible (GBP1), and GBP2[31], were also high. In addition, CCL13, interferon regulatory factor 8 (IRF8), CCR5, VCAM1, HLA-DRA, TYROBP, complement component 1, q subcomponent, B chain (C1QB), major histocompatibility complex class II, DR beta 1 (HLA-DRB1), CD74, and CXCL9 were also upregulated[8,13,14].

Then, a comparative analysis was conducted to determine the extent of the difference between the muscle biopsy and myotube samples (Fig. 2D, Supplementary Table 3). Fifty-three genes were extracted of which 32 (60%) had opposite directions of change in expression (e.g., increased in biopsy vs decreased in myotube). Among the commonly upregulated genes, transmembrane protein 8C (TMEM8C; also known

as a myomaker), myogenin (Myog), and ApoE were found, whereas metallothionein 1E (MT1E) was found among the downregulated genes (Fig. 2E).

Among genes that were commonly altered in muscle biopsies and myotubes, molecules related to muscle differentiation and degeneration were examined at the protein level. TMEM8C is a myoblast fusion-associated molecule[32]. Deletion from myoblasts was reported to exacerbate symptoms in mouse models of muscular dystrophy[33]. The expression of TMEM8C was high in both myotubes and biopsy samples (Fig. 3A, 3B). In immunostaining, the number of TMEM8C-positive myoblasts was higher in sIBM samples than in the control samples (Fig. 3C).

We further investigated ApoE, which accumulates abnormally in sIBM, as a molecule that may be involved in muscle degenerative pathology [18–20]. High expression of ApoE in sIBM was found in the RNA-seq analysis of both myoblasts and muscle biopsies (Fig. 4A, 4B). Immunostaining also showed high expression of ApoE in sIBM (Fig. 4C), as shown previously[18–20]. Furthermore, staining for amyloid oligomer A11 was enhanced in sIBM (Fig. 4D).

Then, we examined the amount of ApoE proteins in myotubes. As expected, ApoE proteins are increased in sIBM compared with control myotubes (Fig. 5A, 5B). In addition, myogenin proteins are significantly increased in sIBM myotubes (Fig. 5A, 5C).

Discussion

In this study, myotubes derived from sIBM-derived myoblasts were established, and RNA-seq was performed to list gene expression profiles solely from myotubes (Tables 2 and 3). By cross-checking the RNA-seq results between the "myotube" and "biopsy" muscle, we could identify TMEM8C and ApoE as commonly altered molecules in the pathogenesis of sIBM myotubes and biopsied muscle (Fig. 2, Supplementary Table 3).

Many of the genes upregulated in the muscle biopsy, which are mostly inflammatory genes, are significantly downregulated in sIBM myotubes compared with control myotubes (Supplementary Table 3). Only 21 genes showed common expression direction changes in both muscle biopsy and myotube samples (Supplementary Table 3). The dissociation of these data can mean that a system based solely on myotubes does not reflect the complicated pathology of sIBM.

Indeed, PSMB8, GBP1, and GBP2, members of the interferon-2 pathway, were increased in biopsy samples, which correlated with previous analyses in the biopsied muscle [31]. The results of the analysis of muscle biopsies suggested altered gene expression in lymphocytes and other immunopathological conditions, which were not involved in the myotube samples. Muscle fibers exhibit persistent senescence-associated secretory phenotype, metabolic disturbances, and cell cycle arrest, which are closely linked to abnormal stimulator of interferon gene (STING), a critical signaling linker protein in intrinsic immune

response [34]. STING activation could be a non-cell-autonomous mechanism of muscle degeneration in sIBM.

Given that changes in skeletal muscle- and myoblast-related molecules such as ApoE and myogenin (Figs. 2, 4, and 5), which have been repeatedly noted in biopsies of sIBM previously[18–20,30], were successfully identified in myotube and biopsied muscle, our analysis may be able to capture intrinsic changes in skeletal muscles in sIBM.

ApoE and lipoprotein receptors are also found in rimmed vacuole structure, suggesting an aberrant cholesterol metabolism in sIBM muscles [19,20]. ApoE stimulates amyloid precursor protein transcription and amyloid beta secretion robustly in human neurons [35]. Amyloid beta-overexpressed mouse was used as the sIBM model[21]. The clarification of the mechanism by which ApoE is high in sIBM myotubes may lead to the control of ApoE-mediated abnormal protein accumulation and muscle degeneration. Previously, we showed that the RNA-binding protein TDP-43 was localized from the nucleus to the cytoplasm in electric pulse stimulation culture[36]. Similar to ApoE, TDP-43 accumulates in the skeletal muscles in sIBM [37]. Patient-derived myotube cells may be useful for the study of the regulation of neurodegenerative disease-related proteins.

TMEM8C, a myomaker, is a well-conserved plasma membrane protein required for myoblast fusion to form multinucleated myotubes [38] [32]. Myogenin is also upregulated in sIBM myotubes[30]. Myogenin binds to the TMEM8C promoter and is required for the expression of TMEM8C and other genes essential for myocyte fusion [39]. Myogenin is also upregulated in sIBM muscle biopsy [30]. In denervation-induced muscle atrophy, myogenin plays both a regulator of muscle development and an inducer of neurogenic atrophy [40]. Given that enrichment analysis also captured changes in muscle contraction and development (Fig. 2B, 2C), the triggering of muscle atrophy signaling and muscle differentiation via TMEM8C or myogenin may be involved in the pathogenesis of sIBM.

This study has several limitations. First, the cell culture condition might have changed the intrinsic gene expression in sIBM myotubes. Single-nuclei RNA-seq using human muscle biopsy could solve the intrinsic gene expression in myotubes *in vivo*. Second, SSC was defined as the control, although it was derived from a pathological joint in the RCT and therefore did not have normal function. Third, the number of sorted cells was dependent on the antibody markers, the specific region of the muscle that was biopsied, and the uniformity and extent of digestion by collagenase. Finally, the number of samples was limited, and various diseases might affect the result.

In conclusion, the results revealed the cell-autonomous profiles of sIBM-derived myotubes. ApoE and TMEM8C are commonly upregulated in both sIBM-derived myotubes and biopsy samples. The catalog of these gene expression changes will be an important resource for future studies on the pathogenesis of sIBM focusing on primary muscle degeneration.

Declarations

Author Contributions

N. Suzuki and M. Kanzaki conceived the project and designed the experiments. M. Koide, R. Fujita, T. Takahashi, K. Ogawa, R. Izumi, Y. Yabe, R. Harada, A. Ohno, H. Ono, K. Ikeda, N. Nakamura, M. Suzuki, S. Osana, A. Warita, Y. Oikawa, T. Toyohara, and M. Kanzaki performed the experiments. N. Suzuki, M. Tsuchiya, T. Abe, R. Nagatomi, and M. Kanzaki analyzed the data. R. Izumi observed muscular tissues by light microscopy. N. Suzuki and M. Kanzaki wrote the manuscript. M. Kanzaki, Y. Hagiwara, and M. Aoki supervised and discussed the experiment. All the authors discussed and revised the manuscript.

Additional Information

Supplementary information accompanies this paper at URL.

Data Availability

The accession number for the RNA-seq data reported in this paper is DDBJ (DNA DataBank of Japan), DRA accession number: DRA017123.

Competing Interests

The authors declare no competing interests.

References

1. Greenberg, S. A. Inclusion body myositis: clinical features and pathogenesis. *Nat Rev Rheumatol* **15**, 257-272, doi:10.1038/s41584-019-0186-x (2019).

2. Suzuki, N. *et al.* The updated retrospective questionnaire study of sporadic inclusion body myositis in Japan. *Orphanet J Rare Dis* **14**, 155, doi:10.1186/s13023-019-1122-5 (2019).

3. Nagy, S., Khan, A., Machado, P. M. & Houlden, H. Inclusion body myositis: from genetics to clinical trials. *J Neurol* **270**, 1787-1797, doi:10.1007/s00415-022-11459-3 (2023).

4. Perez-Rosendahl, M. & Mozaffar, T. Inclusion body myositis: evolving concepts. *Curr Opin Neurol* **35**, 604-610, doi:10.1097/WCO.0000000000001095 (2022).

5. Tanboon, J., Uruha, A., Stenzel, W. & Nishino, I. Where are we moving in the classification of idiopathic inflammatory myopathies? *Curr Opin Neurol* **33**, 590-603, doi:10.1097/WCO.0000000000000855 (2020).

6. Raju, R., Vasconcelos, O., Granger, R. & Dalakas, M. C. Expression of IFN-gamma-inducible chemokines in inclusion body myositis. *J Neuroimmunol* **141**, 125-131, doi:10.1016/s0165-5728(03)00218-2 (2003).

7. Greenberg, S. A., Pinkus, G. S., Amato, A. A. & Pinkus, J. L. Myeloid dendritic cells in inclusion-body myositis and polymyositis. *Muscle Nerve* **35**, 17-23, doi:10.1002/mus.20649 (2007).

8. Greenberg, S. A. *et al.* Highly differentiated cytotoxic T cells in inclusion body myositis. *Brain* **142**, 2590-2604, doi:10.1093/brain/awz207 (2019).

9. Tawara, N. *et al.* Pathomechanisms of anti-cytosolic 5 '-nucleotidase 1a autoantibodies in sporadic inclusion body myositis. *Ann Neurol* **81**, 512-525, doi:10.1002/ana.24919 (2017).

10. Greenberg, S. A. Pathogenesis of inclusion body myositis. *Curr Opin Rheumatol* **32**, 542-547, doi:10.1097/BOR.0000000000000752 (2020).

11. Lloyd, T. E. *et al.* Evaluation and construction of diagnostic criteria for inclusion body myositis. *Neurology* **83**, 426-433, doi:10.1212/WNL.0000000000000642 (2014).

12. Needham, M. & Mastaglia, F. L. Inclusion body myositis: current pathogenetic concepts and diagnostic and therapeutic approaches. *Lancet Neurol* **6**, 620-631, doi:10.1016/S1474-4422(07)70171-0 (2007).

13. Pinal-Fernandez, I. *et al.* Machine learning algorithms reveal unique gene expression profiles in muscle biopsies from patients with different types of myositis. *Ann Rheum Dis* **79**, 1234-1242, doi:10.1136/annrheumdis-2019-216599 (2020).

14. Zhu, W. *et al.* Genomic signatures characterize leukocyte infiltration in myositis muscles. *BMC Med Genomics* **5**, 53, doi:10.1186/1755-8794-5-53 (2012).

15. Zhang, J., Khasanova, E. & Zhang, L. Bioinformatics analysis of gene expression profiles of inclusion body myositis. *Scand J Immunol* **91**, e12887, doi:10.1111/sji.12887 (2020).

16. Cox, F. M. *et al.* A 12-year follow-up in sporadic inclusion body myositis: an end stage with major disabilities. *Brain* **134**, 3167-3175, doi:10.1093/brain/awr217 (2011).

17. Benveniste, O. *et al.* Long-term observational study of sporadic inclusion body myositis. *Brain* **134**, 3176-3184, doi:10.1093/brain/awr213 (2011).

18. Askanas, V., Mirabella, M., Engel, W. K., Alvarez, R. B. & Weisgraber, K. H. Apolipoprotein E immunoreactive deposits in inclusion-body muscle diseases. *Lancet* **343**, 364-365, doi:10.1016/s0140-6736(94)91208-4 (1994).

19. Mirabella, M., Alvarez, R. B., Engel, W. K., Weisgraber, K. H. & Askanas, V. Apolipoprotein E and apolipoprotein E messenger RNA in muscle of inclusion body myositis and myopathies. *Ann Neurol* **40**, 864-872, doi:10.1002/ana.410400608 (1996).

20. Jaworska-Wilczynska, M. *et al.* Three lipoprotein receptors and cholesterol in inclusion-body myositis muscle. *Neurology* **58**, 438-445, doi:10.1212/wnl.58.3.438 (2002).

21. Kitazawa, M., Green, K. N., Caccamo, A. & LaFerla, F. M. Genetically augmenting Abeta42 levels in skeletal muscle exacerbates inclusion body myositis-like pathology and motor deficits in transgenic mice. *Am J Pathol* **168**, 1986-1997, doi:10.2353/ajpath.2006.051232 (2006).

22. Oikawa, Y. *et al.* Mitochondrial dysfunction underlying sporadic inclusion body myositis is ameliorated by the mitochondrial homing drug MA-5. *PLoS One* **15**, e0231064, doi:10.1371/journal.pone.0231064 (2020).

23. Koide, M. *et al.* Retained myogenic potency of human satellite cells from torn rotator cuff muscles despite fatty infiltration. *Tohoku J Exp Med* **244**, 15-24, doi:10.1620/tjem.244.15 (2018).

24. Chen, W. *et al.* In vitro exercise model using contractile human and mouse hybrid myotubes. *Sci Rep* **9**, 11914, doi:10.1038/s41598-019-48316-9 (2019).

25. Bareja, A. *et al.* Human and mouse skeletal muscle stem cells: convergent and divergent mechanisms of myogenesis. *PLOS ONE* **9**, e90398, doi:10.1371/journal.pone.0090398 (2014).

26. Pisani, D. F. *et al.* Hierarchization of myogenic and adipogenic progenitors within human skeletal muscle. *Stem Cells* **28**, 2182-2194, doi:10.1002/stem.537 (2010).

27. Trapnell, C., Pachter, L. & Salzberg, S. L. TopHat: discovering splice junctions with RNA-Seq. *Bioinformatics* **25**, 1105-1111, doi:10.1093/bioinformatics/btp120 (2009).

28. Trapnell, C. *et al.* Differential analysis of gene regulation at transcript resolution with RNA-seq. *Nat Biotechnol* **31**, 46-53, doi:10.1038/nbt.2450 (2013).

29. Suzuki, N. *et al.* NO production results in suspension-induced muscle atrophy through dislocation of neuronal NOS. *J Clin Invest* **117**, 2468-2476, doi:10.1172/JCI30654 (2007).

30. Wanschitz, J. V. *et al.* Expression of myogenic regulatory factors and myo-endothelial remodeling in sporadic inclusion body myositis. *Neuromuscul Disord* **23**, 75-83, doi:10.1016/j.nmd.2012.09.003 (2013).

31. Pinal-Fernandez, I. *et al.* Identification of distinctive interferon gene signatures in different types of myositis. *Neurology* **93**, e1193-e1204, doi:10.1212/WNL.0000000000008128 (2019).

32. Millay, D. P. *et al.* Myomaker is a membrane activator of myoblast fusion and muscle formation. *Nature* **499**, 301-305, doi:10.1038/nature12343 (2013).

33. Petrany, M. J., Song, T., Sadayappan, S. & Millay, D. P. Myocyte-derived Myomaker expression is required for regenerative fusion but exacerbates membrane instability in dystrophic myofibers. *JCI Insight* **5**, doi:10.1172/jci.insight.136095 (2020).

34. Song, C. *et al.* STING signaling in inflammaging: a new target against musculoskeletal diseases. *Front Immunol* **14**, 1227364, doi:10.3389/fimmu.2023.1227364 (2023).

35. Huang, Y. A., Zhou, B., Wernig, M. & Sudhof, T. C. ApoE2, ApoE3, and ApoE4 differentially stimulate app transcription and Abeta secretion. *Cell* **168**, 427-441, doi:10.1016/j.cell.2016.12.044 (2017).

36. Li, Y. *et al.* Feeder-supported in vitro exercise model using human satellite cells from patients with sporadic inclusion body myositis. *Sci Rep* **12**, 1082, doi:10.1038/s41598-022-05029-w (2022).

37. Weihl, C. C. *et al.* TDP-43 accumulation in inclusion body myopathy muscle suggests a common pathogenic mechanism with frontotemporal dementia. *J Neurol Neurosurg Psychiatry* **79**, 1186-1189, doi:10.1136/jnnp.2007.131334 (2008).

38. Di Gioia, S. A. *et al.* A defect in myoblast fusion underlies Carey-Fineman-Ziter syndrome. *Nat Commun* **8**, 16077, doi:10.1038/ncomms16077 (2017).

39. Ganassi, M. *et al.* Myogenin promotes myocyte fusion to balance fibre number and size. *Nat Commun* **9**, 4232, doi:10.1038/s41467-018-06583-6 (2018).

40. Moresi, V. *et al.* Myogenin and class II HDACs control neurogenic muscle atrophy by inducing E3 ubiquitin ligases. *Cell* **143**, 35-45, doi:10.1016/j.cell.2010.09.004 (2010).

Tables

Tables are available in the Supplementary Files section.
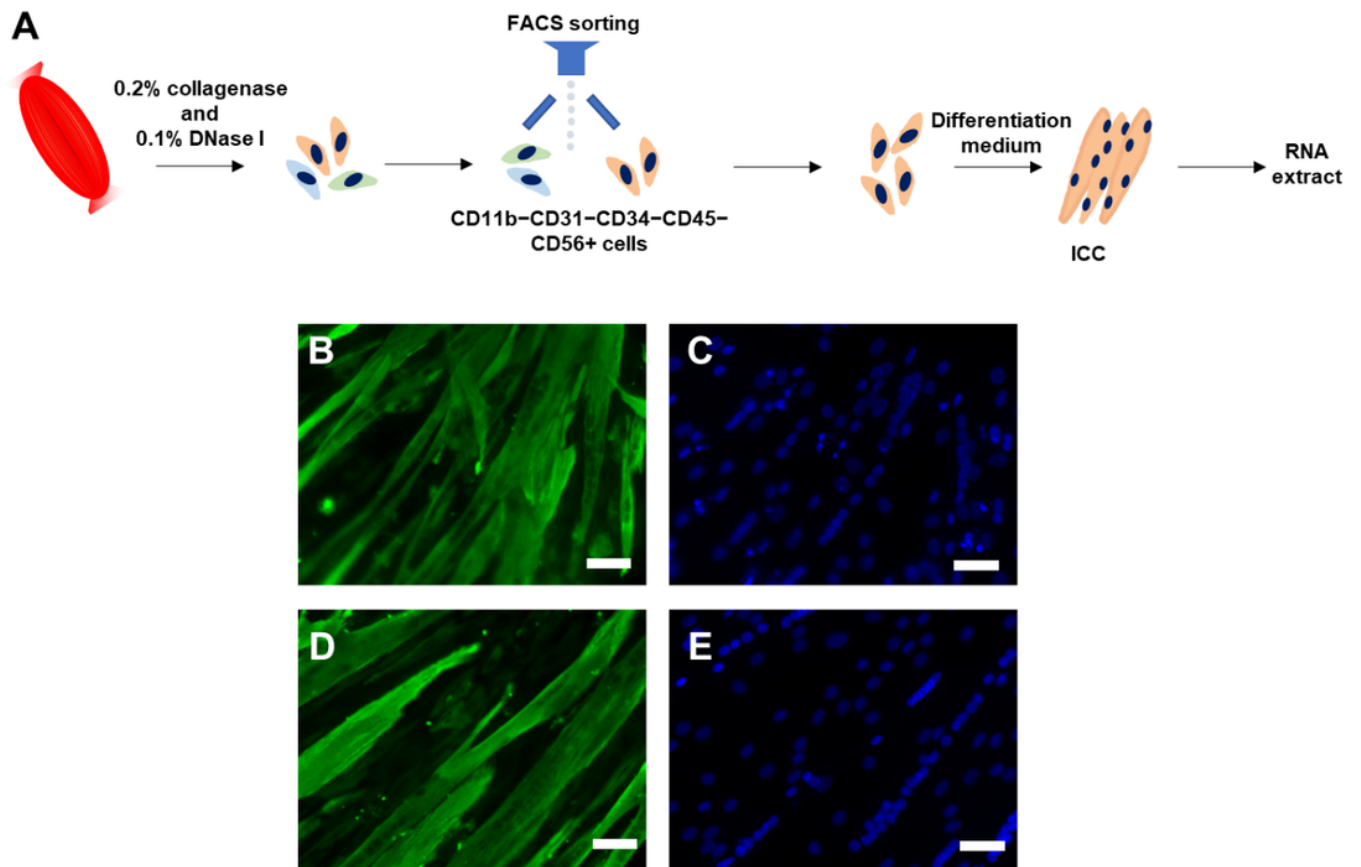
Figures

Figure 1

Figure 1

Myotubes derived from patient muscle biopsy samples

A. Schema of collecting myoblast from the muscle biopsy sample. The tissue was minced and digested with 0.2% collagenase and 0.1% DNase I. CD11b$^-$CD31$^-$ CD34$^-$ CD45$^-$ CD56$^+$ cells were sorted using FACS. Purified myoblasts were expanded in the growth medium. Myoblasts were differentiated into myotubes in the differentiation medium.

B−E. Myotubes derived from patients with sIBM (B, C) and control (D, E). Desmin (B, D) and Dapi (C, E) staining. Scale bar, 50 μm. sIBM, sporadic inclusion body myositis.

Figure 2

A

sIBM control

B

Enrichment Analysis (GO_BP)	# in Category	# Overlaps
muscle filament sliding (go:0030049)	38	18
muscle contraction (go:0006936)	96	13
cardiac muscle contraction (go:0060048)	44	9
skeletal muscle contraction (go:0003009)	23	9
sarcomere organization (go:0045214)	38	7
skeletal muscle tissue development (go:0007519)	44	6
cellular protein metabolic process (go:0044267)	119	6
platelet degranulation (go:0002576)	124	6
transition between fast and slow fiber (go:0014883)	7	5
hydrogen ion transmembrane transport (go:1902600)	59	5
muscle organ development (go:0007517)	84	5

C

Enrichment Analysis (GO_MF)	# in Category	# Overlaps
actin filament binding (go:0051015)	142	13
structural constituent of muscle (go:0008307)	46	10
calcium-dependent protein binding (go:0048306)	60	5

D

991 genes (myotube)   901 genes (biopsy)

53 genes
(*APOE*, *TMEM8C* etc.)

E

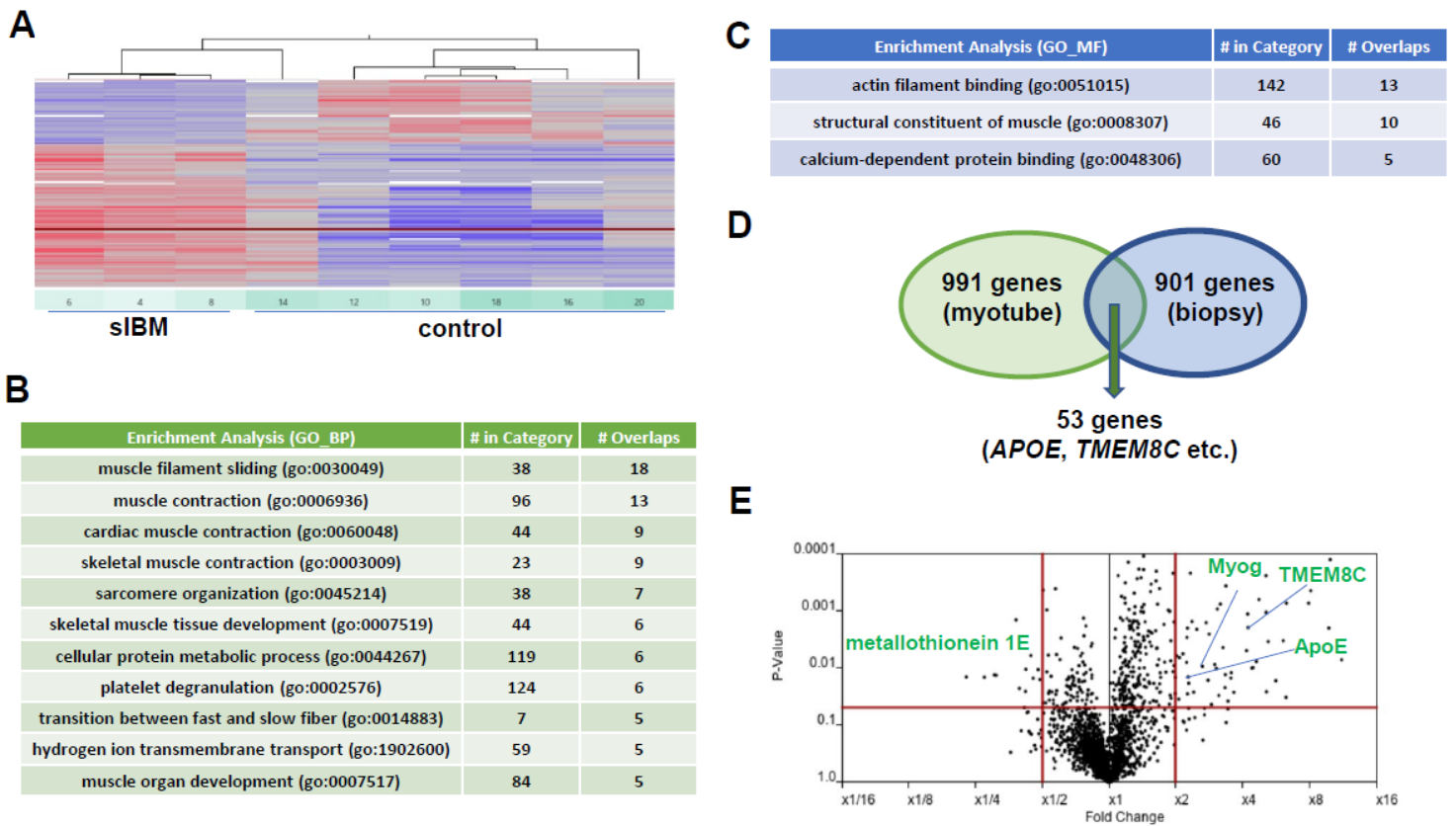Myog. TMEM8C

metallothionein 1E

ApoE

Figure 2

Intrinsic cell-autonomous characterization of myotubes derived from sIBM

A. Heat maps of three sIBM and six control myotube samples.

B. The enrichment of the genes differentially expressed in the sIBM and control groups was analyzed by GO_BP term analysis using the Subio platform. The top terms are listed with >4 overlapped genes, with p-values < 0.05 (Fisher's exact test).

C. The enrichment of the genes differentially expressed in the sIBM and control groups were analyzed by GO_MF term analysis using the Subio platform. The top terms are listed with >4 overlapped genes, with p-values < 0.05 (Fisher's exact test).

D. Venn diagram showing overlapped dysregulated genes between sIBM myotubes (991 genes) and sIBM biopsy (901 genes). Differentially expressed genes (DEGs: fold-change difference of |1.5|) were compared. Fifty-three genes are commonly dysregulated.

E. Volcano plot of the genes differentially expressed in sIBM and SSC focusing genes are plotted on the figures. sIBM, sporadic inclusion body myositis.
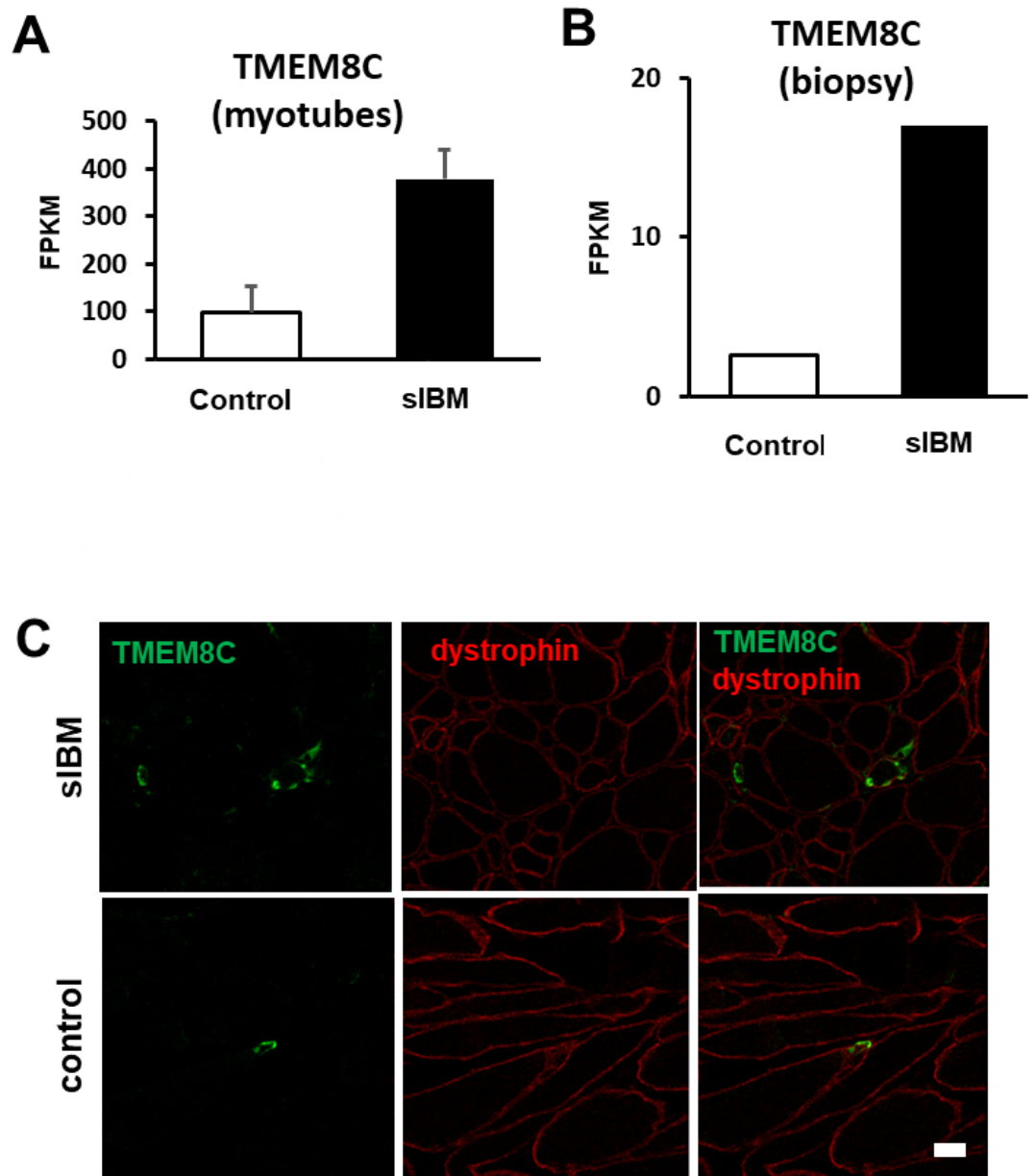
Figure 3

Figure 3

Expression of TMEM8C in both myotubes and sIBM biopsy sections

A. TMEM8C mRNA upregulation in sIBM myotubes.

B. TMEM8C mRNA is upregulated in the sIBM biopsy muscle.

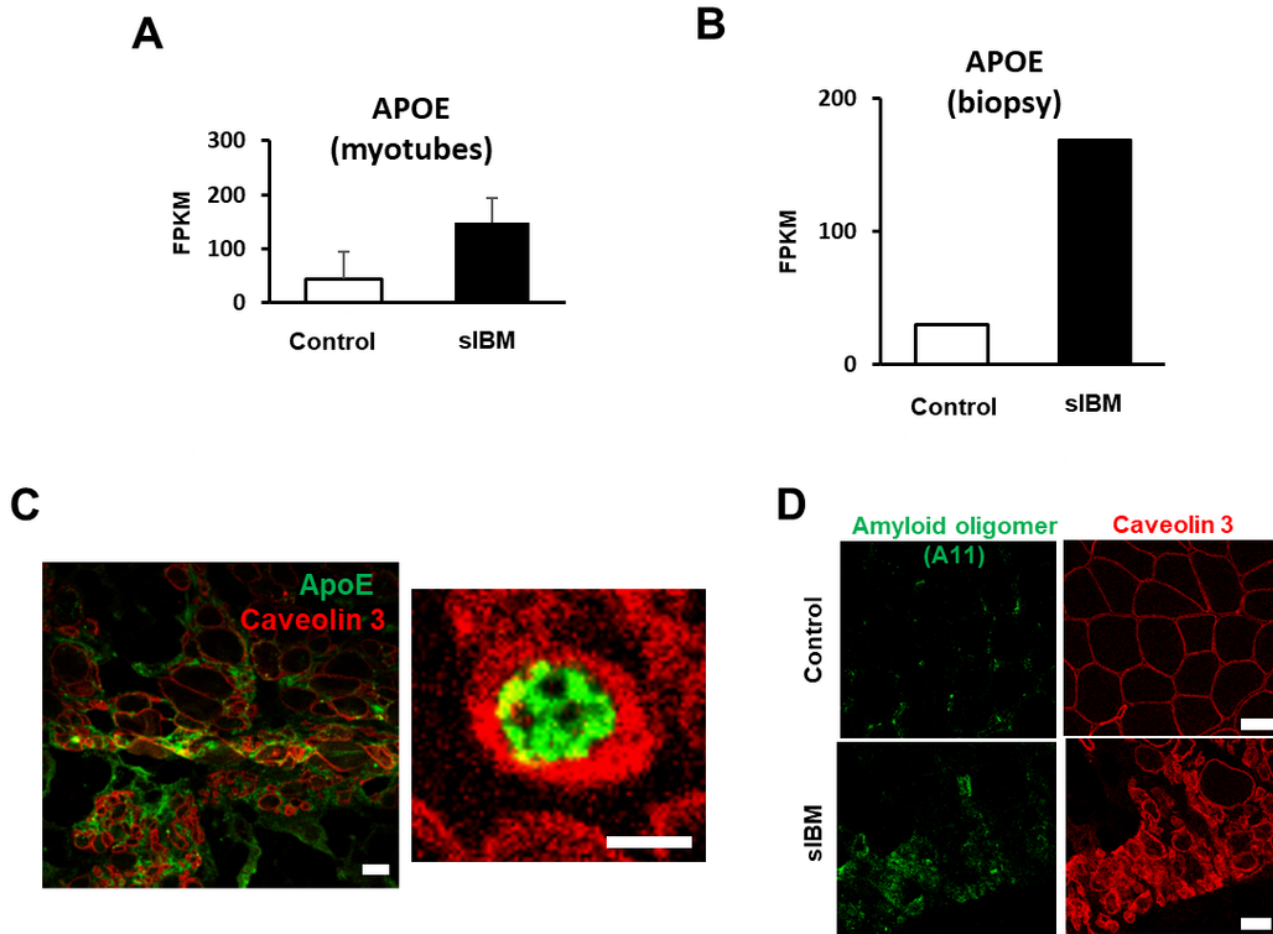C. TMEM8C is found in the sIBM biopsy section. Scale bar, 10 μm.

Figure 4

Figure 4

Expression of ApoE in sIBM biopsy sections

A. ApoE mRNA upregulation in sIBM myotubes.

B. ApoE mRNA is upregulated in the sIBM biopsy muscle.

C. ApoE protein is upregulated in the sIBM biopsy section. Scale bar, 10 μm.

D. Amyloid oligomer (A11) is upregulated in the sIBM biopsy section. Scale bar, 50 μm.
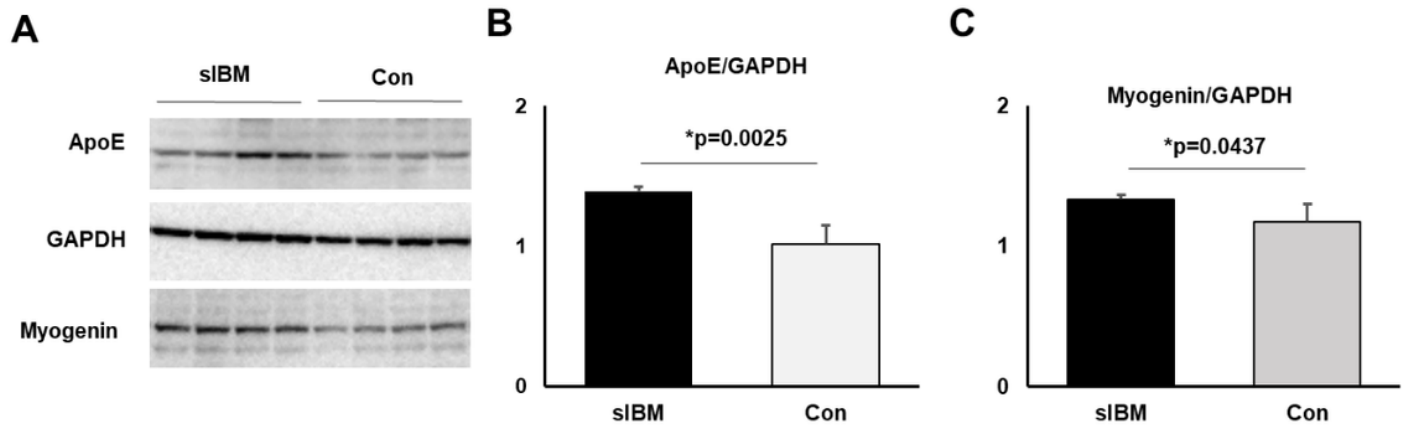
Figure 5

Figure 5

Protein levels of ApoE and myogenin in sIBM myotubes

A. Representative blot of ApoE, GAPDH, and myogenin in sIBM and control myotubes.

B. The protein level of ApoE is significantly increased in sIBM. P = 0.0025. Students' t-test.

C. The protein level of myogenin is significantly increased in sIBM. P = 0.0437. Students' t-test.

Supplementary Files

This is a list of supplementary files associated with this preprint. Click to download.

- 231010SciRepsIBMmyoblastSuppleLegendsFigureTables.pdf
- 230826SciRepsIBMmyoblastTables.pdf